Proceedings of the IASS 2024 Symposium
Redefining the Art of Structural Design
August 26-30, 2024, Zürich Switzerland
Philippe Block, Giulia Boller, Catherine DeWolf,
Jacqueline Pauli, Walter Kaufmann (eds.)

Compression response of digitally manufactured engineered bamboo spliced hollow columns

Phillip J.S. RUSSELL, Dan V. BOMPA*

School of Sustainability, Civil and Environmental Engineering, University of Surrey, GU2 7XH, UK
d.bompa@surrey.ac.uk

Abstract

Bamboo is increasingly being considered as a viable alternative to established construction materials due relatively low environmental impact and adequate mechanical properties. This material has been adopted in construction, both in its natural state and in engineered form for structural elements. However, its mechanical performance is not fully evaluated. This paper examines the experimental response of Engineered Bamboo (EB) rectangular hollow section columns that incorporate flat panels connected by through tenon dry mechanical connections. Columns with various slenderness ratios were designed and digitally fabricated from EB planks. After assembly, these specimens were subjected to axial compression testing alongside complementary material tests. In addition to conventional measurements, a two-dimensional Digital Image Correlation system was employed to evaluate the strain behaviour throughout the testing regime of these samples. Test observations indicate that the failure of the columns was related to the shear dislocation of the faces, predominantly through the shear of the tenons. However, splitting of the mortise sections was also noted. This brittle response was characterized by lateral dilation of the column and buckling of the EB plates, leading to complete collapse. These results provide a detailed insight into the structural performance of digitally manufactured hollow EB columns, which can be employed in temporary lightweight structures that are designed to be disassembled and reused.

Keywords: digital manufacturing, engineered bamboo, dry mechanical connections, compression members

1. Introduction

Bamboo grows faster than timber and it is naturally found in many developing countries where small-scale construction developments are expected within the foreseeable future [1,2,3]. To eliminate the high variability in material properties of natural bamboo [4,5,6], EB is an alternative by forming standardised panels from bamboo fibres and resins [7,8]. EB is produced either in laminated or densified forms. Laminated bamboo is commonly used for sheeting solutions, and both densified and laminated solutions being common amongst other uses [1]. Laminated Bamboo Lumber (LBL) is manufactured by splitting the natural bamboo culms into pieces, which are stripped of their outer and inner layers, and are then flattened to form rectangular batons and bonded with adhesives in layers [8]. EB preservation involves bleaching or caramelisation with different effects on the material [1]. LBL mechanical properties are linearly related to the fibre density of the material [9], with the tensile capacity perpendicular to the grain being 30 times lower than that parallel to the grain [10].

Previous research showed that square hollow section columns can be fabricated by bonding panels of LBL panels together using adhesives [11, 12]. Tests on columns with various slenderness ratios and wall thicknesses for columns, showed that each grouping had differing modes of failure, with the short members crushing and the long members experiencing elastic buckling [11]. The intermediate columns experienced a range of failure modes, including splitting, crushing and inelastic buckling [11]. Moreover, Ref. [7] indicated that local failure is more typical in box sections before the complete section

failure. In this case shear dislocation resulting from shear displacement was the most dominant cause towards ultimate failure, with the dislocation parallel to the loading axis, with the displacements perpendicular to this [7]. The bearing capacity of the columns reduced with increase in slenderness due to plate buckling and subsequent shear dislocation or delamination of the glued layers [7,12,13].

As an alternative to bonding with adhesives, dry mechanical connections (DMC) also referred to integral mechanical attachments, can provide tying between two neighbouring EB plates, but also potential for disassembly and reuse. Whilst DMCs have been explored for timber-timber joints [14,15], such connection types have not been explored for bamboo composite [16]. Investigations on plywood and other engineered wood product DMCs, indicated that the both the insertion angles and primary grain direction influence the strength of the connection [14]. Cross-plies aid the resistance of the section, and DMCs connected perpendicular to the grain provide more ductility compared to parallel grain [14]. Tests on dovetail joints indicated that the main failure modes were shear of the dovetail and tensile splitting of the wood [17]. Regarding detailing of dovetail joints, a neck width of 7-15 mm with a tenon angle of 56-63° gives optimum response. Similar experiments indicated that grouting a clear gap between positive and negatives of the teeth of the dovetails enhances joint the stiffness [18].

The recent development and popular return of DMCs for timber structures relates to the increased use of CNC machines. These are beneficial due to the speed and ease of precise construction and assembly, allowing for the simplification of complex design [19]. The growth of use of DMCs is beneficial for structural use [16]. As noted above, these techniques have been used for timber DMCs, but not for EBs. Bamboo tends to be inherently more brittle compared to timber, both in natural and engineered forms, posing challenges in employing in DMCs, both regarding digital fabrication and structural response. The compression behaviour of EB columns incorporating DMCs, including stiffness, strength and deformability has not been evaluated before.

In this paper, LBL planks, typically used for flooring were digitally cut, spliced, and connected by DMCs to form hollow section columns. Dovetail joints were used to splice the LBL panels along the longitudinal directions, and through tenon and mortise joints transversally to connect the corners of the box columns. Additional steel brackets are used to connect two LBL panels together to form a column side. This fabrication approach enables the development of columns with variable slenderness, which are then tested under axial loading. Column tests are complemented by material tests to evaluate the fundamental mechanical properties of the EB. In addition to conventional measurement, two-dimensional Digital Image Correlation (2D-DIC) [20] techniques were used to evaluate stress distributions and concentrations at the column face and DMCs. These results provide a detailed insight into the structural performance of digitally manufactured hollow EB columns which can be employed in temporary lightweight structures that can be disassembled and reused.

2. Materials and methods

2.1 Materials

Bamboo is a fibrous material, meaning that its mechanical properties are directly linearly related to the fibre density of the material, and are dependent on the direction of the fibre with respect to the loading [19]. As well as the fibre density, the production methods used to manufacture the engineered bamboo (EB) sections influences the structure of the section [1,8]. To evaluate the main mechanical properties, compression, tension, and shear tests were carried on samples extracted from rectangular EB floorboards. The floorboards were 15 mm thick, and 96 × 960 mm in plan, including a tongue and groove joint and 1 mm ribbing on the underside of the board. These included three layers without cross-lamination, with the fibres ran parallel to the length of the board. The engineered material included around 93% bamboo strips (lignin/cellulose) and 7% glue, had a nominal density of 1150 kg/m^3, a modulus of elasticity of 12090 N/mm^2 and a bending strength of 99.6 N/mm^2 to EN 408. The moisture content was 2.03±0.61%, obtained through existing guidance.

To evaluate the fundamental mechanical properties of the EB materials used in the research, compression, tension and tenon shear tests were carried out (Figure 1). For the compression tests, 3 × 200 × 67 × 45 mm^3 prismatic samples made of three 14 mm panels tied with water-resistant wood glue

were manufactured, as guided by EN 789. The glossed top surface of each plank was sanded before gluing to provide enhanced bond. The compression samples were used to determine the stress-strain response, elastic modulus, and compressive strength. To evaluate the uniaxial tension capacity, 3 × dog-bone specimens with a length of 500 mm, an end cross-section of 80 × 14 mm and a middle section of 48 × 14 mm, were also tested. These dimensions are a scaled version of those set out in EN 789, due to the limitations imposed by the size of a plank. To evaluate the shear resistance parallel to the fibre of the outer layers, 3 × 48 × 14 mm tenon shear tests were carried out. These tests give an insight into the shear behaviour of the tenons and would inform the design of the number and size of elements to ensure sufficient connection capacity between planks. In addition to the engineered bamboo, galvanised steel brackets and 4 mm bolts were used for transverse mechanical fixing of the EB boards.

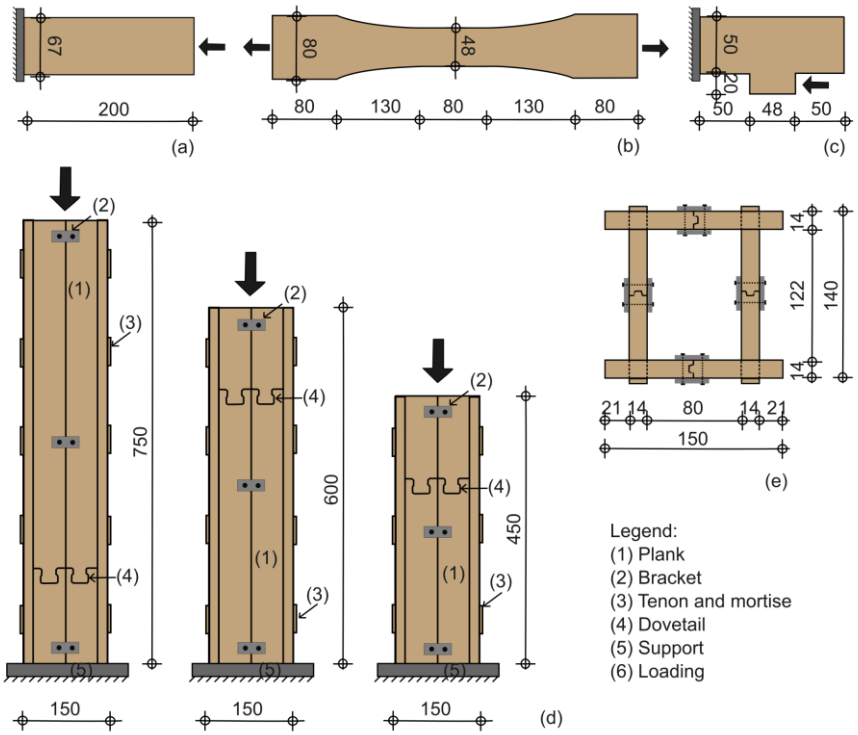

Figure 1: Schematic representation of the: a) compressions tests on prisms, b) dog-bone specimens in tension, c) tenon shear tests, d) column specimens, e) column cross-section.

2.2 Specimen details

To evaluate the slenderness effects on the response of EB columns with DMC, six specimens with box section of 140 × 150 mm, representing a section size that can be considered suitable for structural applications, were designed, and fabricated as shown in Figure 1. The columns used the above EB planks with a plate thickness t=14 mm and had three distinct lengths l=450, 600 and 750 mm. For infinitely long material 14 mm sheet, the columns would have a total of 4 × 150 mm plates of the above lengths joined at corners by means of DMC in the form of tenon and mortise joints. Due to width limits imposed by the size of the floor planks, in addition to the corner DMCs, splicing along the length/longitudinal direction and width/transverse direction was needed.

Regarding the jointing of corners, tenon and mortise joints were selected for their ease of production using the CNC cutting machine and in their fabrication process. There is no significant literature relating to the sizing of depths of tenons and the spacing between such joints, hence these values were taken as 50 mm tenon depth and 100 mm clear spacing between tenons was selected, similar to values adopted in existing literature [14,15]. It is worth noting that despite the poor performance of tenons at 90^{o} to the side face of a plate in shear, there was minimal choice in the matter when considering a follow-up investigation into these same sections in tension. This is due to the heightened possibility of pull-out of inclined tenon-mortise connections.

For the longitudinal splicing of the EB boards, dovetail joints were considered. Although under loading these splices would be in compression, the dimensions of these were selected to provide the highest strength in tension and had near zero clearance, providing appropriate tightness to reduce the chances of hinges developing under plate buckling. Longitudinal splices were designed to lie at the midspan between tenons and staggered around the column in a helical fashion. Consequently, the 450 mm and 600 mm columns had two and one face respectively without any splices.

Prototype cuts were carried out to determine the feasibility of the EB joints that would be used. In this initial stage, joints were designed to have teeth 0.5 mm larger than the gap which they would fit in for the dovetailed joints, and tenons were designed to be 1.0 mm larger than the mortise. This was considered to provide a tighter joint and ultimately increase the strength of each joint. Joints made using these tolerances split along the grain. Consequently, the teeth were sized down to match the size of the negative in its opposite member, and in some instances adjusted by sanding up to a final tenon depth of 49 mm. Due to the cutting tool bit being rotary, 8.0 mm diameter notches were formed at all concave corners, including the tenon-side face and in the corners of the mortises.

For transversal tying different approaches were developed for the mechanical fixing of two boards to allow for wider widths of column, because the tongue and groove joint was not rigid and tight enough. An internal EB diaphragm or EB C-shaped brackets were considered and manufactured, yet these split along the grain due to the low in-plane shear strength of the material. Finally, 25×15×2mm zinc plated steel brackets and 4 BA (4 mm) roundhead bolts in 5 mm drilled holes were considered for tying two planks together. Due to the relative size and material properties of the steel elements, these would act as rigid elements, ensuring sufficient tying capacity. The brackets were positioned symmetric to the mid-height of the columns and the number of brackets was as a function of the column length. These were positioned on both the internal and external faces, using washers.

2.3 Fabrication

For the fabrication of the sections, the CNC cutting machine was set up to cut planks in pairs. The planks were secured using screws to the sacrificial MDF panel. Each section was cut considering 7 passes, including a 1 mm final pass to provide a smooth finish to the reverse face, with CAD converted into a cutting template using VCarve software. Additionally, tabs of 5 mm thick and 10 mm width were used to hold each piece in place whilst the machine finished cutting, using an 8 mm rotary bit. To ensure uniformity in the cutting process, the origin point for the cutting bed was considered at the corner of the meeting grooved edges of the bamboo, as opposed to that of the tongued edges.

A chisel and rubber mallet were used to break off all the tabs from the cut panels before using the rubber mallet to join the splices together to form each face. The mortises were sanded to provide a wider entrance on the back face, prohibiting shear failure of tenons in the assembly process. Then the corners were assembled by using the rubber mallet in two stages, initially by partly inserting the tenons into the mortises, and then the final 5 mm all the way through to produce the joint. This process minimised any bending on the dovetail joints which could have produce failure during the assembly. Due to limited tensile strength of EB and lack of cross-lamination discussed, tenon shear, dovetail splitting (bamboo – failure through each layer of culms), dovetail splitting (resin – failure in the joint between two bamboo culms), mortise splitting (bamboo) and mortise splitting (resin), occurred during assembly.

Before testing, all the specimens, including columns and material tests were measured to give their final sizes. This was carried out by using digital callipers (accuracy of ±0.01mm) to determine the widths and depths of members, and a meter rule with an accuracy of ±1.0 mm to measure the heights. Each measurement was taken three times at varying locations along the specimen and was subsequently averaged. One face of each column was spraypainted white to provide a plain background that is easy to contrast against for detailed DIC assessments. After two to three coats, the faces were left to dry before they were stamped with a black ink dotted pattern. Additionally, reference gauges with lengths of 100 mm were dotted onto the same face, using a red marker, for DIC scaling.

2.4 Testing arrangements and instrumentation

An Instron 600 kN testing machine was used for the compression members. The machine was fixed to the ground and applied load to the top of the specimens at a displacement rate of 1.0 mm/min to failure. Before starting testing, the specimen was placed in the press atop a steel plate, with a second steel plate placed on top to distribute the load evenly (Figure 2). To avoid any eccentricity introduced into the sample, the specimen was centred under the head of the hydraulic press provided with a hinge. This method was repeated for all six columns and four compressive prism tests. The three tensile and three shear tests were carried out in an Instron 8802 machine at a displacement rate of 1.0 mm/min.

To evaluate strain development and surface displacements, an in-house digital image correlation (DIC) was used. This DIC adopted a non-contact system that uses one high-sensitivity APS-C type (23.5 × 15.6 mm), Exmor CMOS sensor camera with USB 3.0 interface to provide accurate and practical measurements for material and specimen tests. The camera had a resolution of 24.2 Megapixel and was set to take repeated pictures at 10s intervals until stopped manually. A Perspex sheet was then placed in front of the specimen, to avoid damage to the camera, and additional photos were taken of the specimen to show the general arrangement. Throughout each test, notes were taken regarding the behaviour of the specimen, and additional pictures were taken to show the relevant failure mechanisms from all sides.

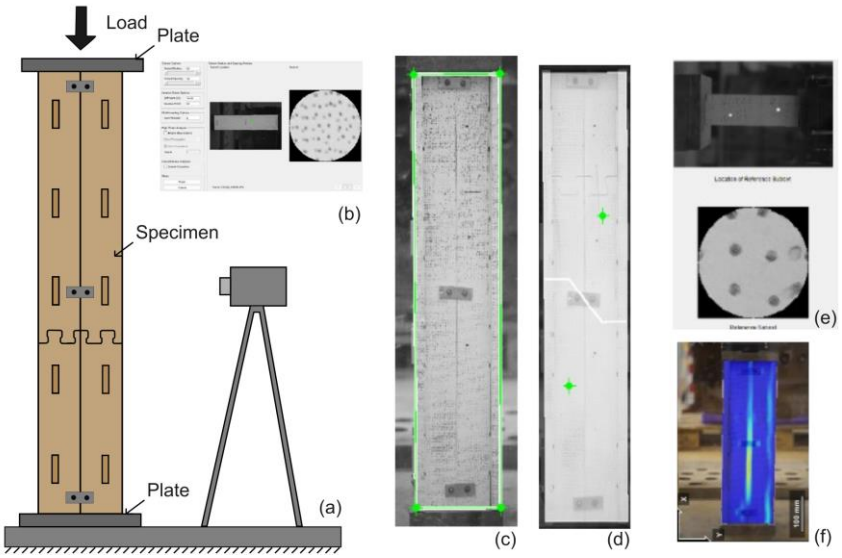

Figure 2: Schematic representation of the testing arrangement; DIC processing flowchart: b) subset selection, c) field of view, c) selection of scaling points, d) scaling, e) strain maps.

An open-source 2D-DIC tool [20], was employed for analysis for all specimens. The process involved selecting tasks from the program state list (Figure 2). A reference image was captured prior to each test, serving as a baseline for subsequent images. After loading the reference image, all test images were imported. The Region of Interest (ROI) was defined as the specimen polygonal shape from the reference image. Analysis parameters were set, including maximum subset radius, spacing, and two threads for seed selection. Analysis began by selecting the ROI and two seeds for tracking. Displacement and strain scaling followed analysis, using inked points at a known distance apart. The strains were then correlated by ensuring the strain radius was small enough to not include significant discrepancies across the circle. Post-processing adopted the Ncorr post-processor [21] adopting virtual extensometers after scaling. Longitudinal and transverse strains were then computed along two defined gauges in each direction.

3. Results and comparative assessments

3.1 Material tests

To evaluate the stress-strain response of the LBL material in compression, the DIC data and machine recordings were used. The machine load was divided by the sample section to obtain the stress and compressive strength, whilst the DIC for strain measurements. From the stress-strain response, relevant

values for this material, including elastic modulus and maximum compressive strength have been evaluated. The measured compressive strength obtained from four tests was f_{Lc}=41.3±3.2 MPa. Figure 3a shows the overall constitutive response evaluated from the DIC data. It is shown that the response is characterised largely by a bi-linear response with hardening, with a yield point around 30 MPa. The crushing strain corresponding to peak strength was around 2.14% and a failure strain above 2.5%. As indicated in Figure 3d, the failure occurred due to fibre crushing and debonding of the three plates.

Figure 3b shows the tensile stress-strain curves and typical representations of the dog-bone specimens after testing. The stress was evaluated by dividing the machine recorded force by the smallest cross-section of the sample, whilst the strain was evaluated from DIC data using a gauge length of 80 mm. From Figure 3b, it is shown that the response is largely characterised by a bilinear response with an elastic linear branch between 0 and 40 MPa, and a second linear branch from around 40 MPa to ultimate strength. The average tensile strength exhibited by the LBL specimens was 81.4±9.4 MPa. The failure of two was mainly dictated by longitudinal shear between the laminated batons, hence the failure induced in the resin (Figure 3e). The remaining specimens failed in a ductile tensile manner (with some longitudinal shearing intermixed between the shearing of batons).

Figure 3c illustrates the shear test outcomes. The maximum peak shear stress recorded was 7.48 MPa at a displacement of 0.9 mm, whilst the minimum peak shear stress was 5.92 MPa at 5.9 mm. The shear stress was obtained by dividing the load recorded by the machine by the section of the tab/tenon. On average, the shear strength was 6.71 MPa with a standard deviation of 0.78, indicating some variability. Regarding specimen behaviour, all specimens failed in a brittle manner, through a vertical crack appearing at the root of the tab/tenon. This is evidenced by the linear stress-displacement curve shown in Figure 3c, which shows a sudden drop in stress after the peak, and Figure 3f indicating a splitting crack without other forms of failure.

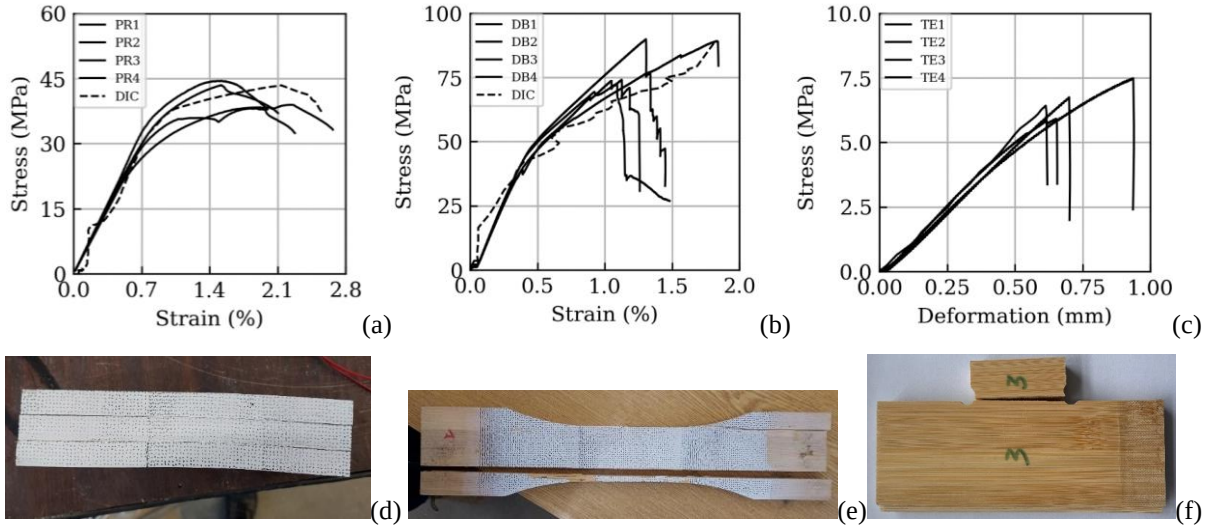

Figure 3: a) compression stress-strain curve, b) tension stress-strain curve, c) tenon shear stress-deformation curve; samples after failure: d) prism in compression, e) dog-bone sample in tension, f) tenon sample in shear.

3.2 Column tests

The load-shortening curves of the column tests are shown in Figure 4. The curves are characterized by a linear elastic branch with some softening around 70-80% of the peak capacity, and a sudden drop in strength after peak. It is shown that the response in compression was brittle without sign of ductility. For the short columns (CS1 and CS2), the secant stiffness K measured at 40% of the peak capacity P_u was on average 73.5±2.0 kN/mm, whilst the peak capacity was 229±3.1 kN. For the intermediate size members (CM1 and CM2), K was 68.9±5.2 kN/mm and P_u=245±22 kN. For taller members (CH1 and CH2), K=63.9±1.5 kN/mm and P_u=234±16 kN. It is shown that the secant stiffness tends to decrease with increase in height, as expected. The increase in plate slenderness permits for larger deformations

for the same applied load. The ultimate capacity is largely the same for all members regardless of their slenderness. This is due to strain localisation at DMCs and local brittle failures.

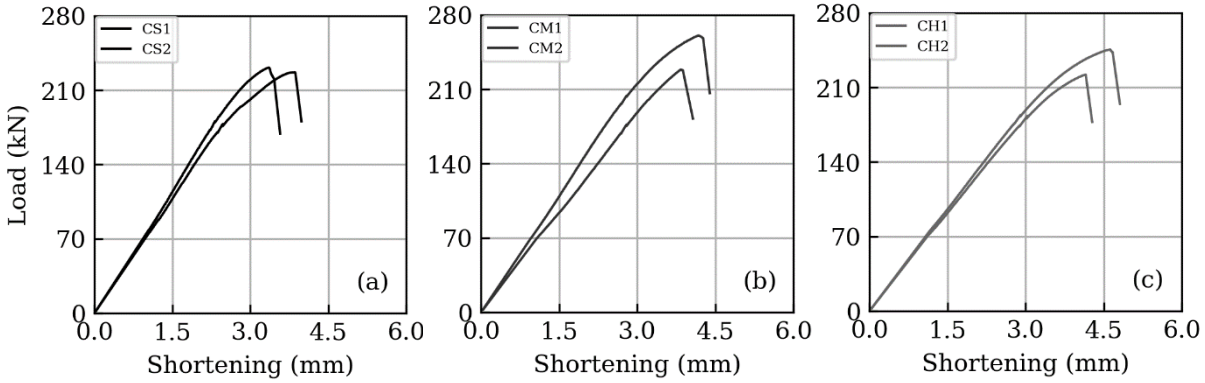

Figure 4: Load – shortening curves for: a) CS specimens, b) CM specimens, c) CH specimen.

The DIC processing permitted the evaluation of strain maps and distributions across one face of the column specimens, enabling an understanding of strain localisation and failure kinematics. The initial data from the DIC was used to correlate the stress-strain relationships of the columns. The stress corresponds to the load divided by the cross-sectional area of the box section, whilst the strain extracted using virtual gauges from the DIC measurements. Figures 5,6,7 illustrate the above parameters for the tested columns. Figure 5a, 6a, and 7a plots the longitudinal strains for the CS, CM and CH members, respectively, at three distinct load levels (i.e. notation a, b, c after specimen name indicates strains at around 15%, 50% and 95% of the peak load P_u). Figures 5b, 6b, and 7b shows the transverse strains for CS, CM and CH members, respectively, whilst Figures 5c, 6c, and 7c strain maps for the same members. It is generally shown that longitudinal strain localisations are associated with the dovetail joints, and that the largest transverse strains are at the tongue and groove joints but restrained by the steel brackets.

Experimental observations showed that the elements with greater slenderness tended to fail brittlely, whereas the stockier elements failed more in plate buckling. Yet, the governing failure mode was through shear of the tenons leading to a shear dislocation similar to observations from the literature [7]. This is equally evident when considering the consistency of tenon shear and mortise splitting failure throughout the test specimens, which can clearly be seen in the images taken after testing in which every tenon had cracks or failed (Figure 8). It was shown that there was also damage sustained to the other areas of the specimens. The explanation that failure of the columns is reliant on the shear capacity of the tenons is reinforced when comparing the maximum stresses seen in the specimens to the ranges [8]. This is also evident when considering all the columns failed at similar peak load capacities, regardless of their slenderness. Thus, for an enhanced capacity, the tenon and mortise connections would need to be proportionately designed. Provided that the failure at the dry joints is avoided, the behaviour would be governed by plate buckling.

This shear dislocation can be also observed in the strain profiles obtained from the DIC analysis in both the lateral strain distributions and the lateral strain diagrams, with significant peaks consistently occurring at the through tenon joints and increasing with the application of load (Figure 5, 6, 7). It must also be noted that peaks also occur along the tongue and groove joint although this was expected for the reduced rigidity of this connections due to the mechanical fixings having 1-2 mm clearance in the positioning of bolts, allowing for lateral movement. This condition led to some movement and strain localisation around the dovetail joints, increasing through testing. This means that the gaps inherent in the assembly of the sections closed gradually as loading increased, relating to the rapidly increasing strains at low stresses for most of the column tests. These local strains then continued to grow throughout testing as the bearing on the splice did cause localised damage, without failure, from bearing action.

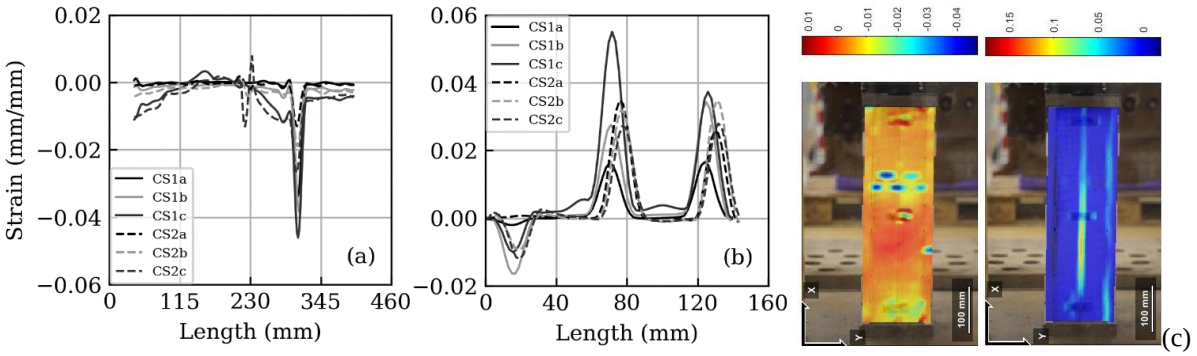

Figure 5: Strain profiles and maps for CS specimens: a) axial strains, b) transverse strains, c) strain maps (axial strains at left, transverse strains at right).

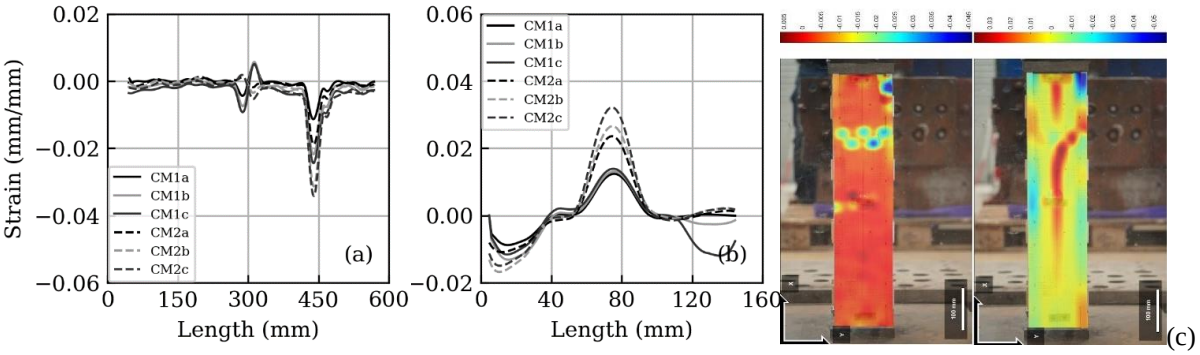

Figure 6: Strain profiles and maps for CM specimens: a) axial strains, b) transverse strains, c) strain maps (axial strains at left, transverse strains at right).

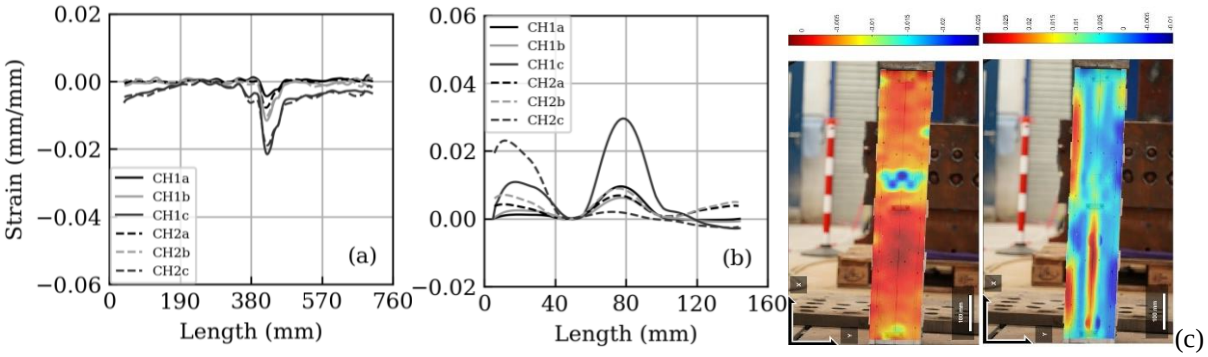

Figure 7: Strain profiles and maps for CH specimens: a) axial strains, b) transverse strains, c) strain maps (axial strains at left, transverse strains at right).

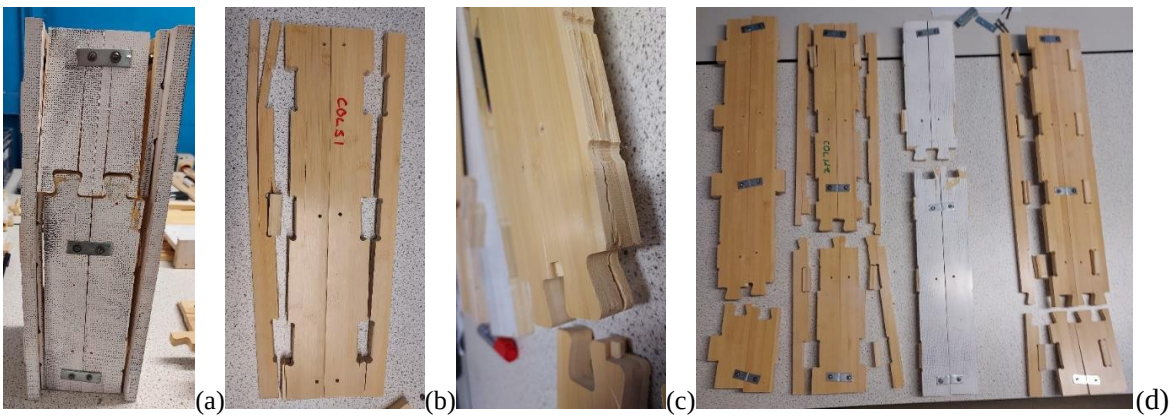

Figure 8: Specimens after failure: a) CS specimen with out-of-plane dovetail joint deformations, b) splitting along the tenon and mortise joint, c) splitting of the bamboo lamellae at the dovetail joint, d) CH specimen after testing.

This study showed that for engineered bamboo with mono-directional fibre orientations, the structural response of box columns highly depends on the relationship between loading direction and grain orientation [16]. Ideally the tenons are orientated in the primary grain direction [14], yet this was not possible here due to the orientation and dimensions of the boards supplied. Whilst, changing the direction of the fibre regarding tenon location, changing the grain direction would reduce the maximum axial capacity as the compressive strength of bamboo is lower perpendicular to the grain rather than parallel [8]. Cross-laminations with a higher number of layers and nearly equal by both directions, would provide an enhanced mechanical property. Dovetail joints used for splices offer a viable option, but their inherent nature allows for flexibility at the connection area, facilitating strain concentration that becomes increasingly apparent with higher axial loads and out-of-plane plate deformation.

4. Concluding remarks

The experimental response of Engineered Bamboo (EB) rectangular hollow section columns, incorporating flat panels connected by through tenon dry mechanical connections (DMCs), was examined in this paper. Columns of various slenderness ratios were designed and digitally fabricated from EB planks. After assembly, these specimens underwent axial compression testing alongside complementary material tests. A two-dimensional Digital Image Correlation (DIC) system was employed to assess strain localisation and failure kinematics. The main remarks are outlined below.

EB material exhibited a bi-linear stress-strain response in compression, with a yield point around 30 MPa, and a peak compressive strength of 41.3 MPa. In tension, EB specimens showed an elastic linear branch up to 40 MPa, followed by a second linear branch to ultimate strength, with an average tensile strength of 81.4 MPa. Shear tests on LBL showed an average shear strength of 6.71 MPa. Compression prisms failed by crushing with debonding, tension failures were by longitudinal shear between laminated batons, and shear tests appeared through a vertical crack at the root of the tenon.

Column tests showed a linear elastic response followed by softening around 70-80% of peak capacity, with a sudden strength drop after peak. For short columns, the secant stiffness at 40% of peak capacity averaged 73.5 kN/mm, with peak capacity at 229 kN; intermediate size members showed 68.9 kN/mm stiffness and 245 kN peak strength, whilst taller members had an average stiffness of 63.9 kN/mm and 234 kN strength. The results indicate stiffness decrease with height increase, whilst the ultimate capacities remained consistent across members due to strain localisation and local brittle failures.

Experimental observations indicate that slender columns tend to fail brittlely while stockier elements fail in plate buckling, with shear cracking and dislocation of tenons being the governing failure mode. Strain profiles from DIC analysis showed significant peaks at dovetail joints, at through tenon joints, as well as some level of localisation at tongue and groove joints but minimised by steel brackets. It is shown that the overall behaviour of the configurations investigated in this paper is governed by the geometry of the tenon and mortise DMCs, as well as the orientation of the EB grain with respect to loading.

Acknowledgements

The authors gratefully acknowledge the support provided by the technical staff at the University of Surrey, particularly Dr Surya Biswal, Ms Thabang Ntanda and Mr Hayder Abedi with digital manufacturing and testing of the specimens described in this paper.

References

[1] B. Sharma, A. Gatóo, M.H. Ramage, “Effect of processing methods on the mechanical properties of engineered bamboo”. *Construction and Building Materials*, vol. 83, pp.95-101, 2015.

[2] E.Z. Escamilla, G. Habert, H.A. Santos, J.S.E. Fernández, D. Trujillo, “Industrial or traditional bamboo construction? Comparative life cycle assessment (LCA) of bamboo-based buildings.” *Sustainability*, vol. 10(9), p.3096, 2018.

[3] L. Mbereyaho, J. de Dieu Mutabaruka, A.G. Gershome, A. Ineza, E. Ngirabatware, “Strength, sustainability and affordability of bamboo and mud bricks as materials used in local construction.” *Rwanda Journal of Engineering, Science, Technology and Environment*, vol. 2(1), 2019.

[4] A. Azadeh, K. Ghavami, H. Savastano Junior, R.D. Toledo Filho, N.P. Barbosa, "Static flexural behavior of bamboo as a functionally graded material and the effect of heat on dynamic flexural modulus." *Journal of Building Engineering*, vol. 34, p.101949, 2021.

[5] A. Azadeh, A.D. De Sá, M. Kadivar, C. Gauss, H. Savastano Junior, "The effect of densification on physical and mechanical properties of bamboo Dendrocalamus asper." *European Journal of Wood and Wood Products*, vol. 80(4), pp. 877-888, 2022.

[6] D.V. Bompa, S.A. Behnejad, H. Savastano Junior, A. Azadeh, M. Pourghaz, "Experimental evaluation of load-induced cracking in moso bamboo tubes." *In Proceedings of IASS Annual Symposia*, 2023.

[7] Y. Su, J. Zou, W. Lu, "A macroscopic shear angle model for ultimate bearing capacity of glued laminated bamboo hollow columns under axial compression." *Structures*, vol. 45, pp. 560-571, 2022.

[8] B. Sharma, A. van der Vegte, *Engineered bamboo for structural applications. In Nonconventional and vernacular construction materials.* Woodhead Publishing, 2020.

[9] Y. Xiao, R.Z. Yang, B. Shan, "Production, environmental impact and mechanical properties of glubam." *Construction and Building Materials*, vol. 44, pp.765-773, 2013.

[10] A. Azadeh, A.Q. Flores, K. Ghavami, N.P. Barbosa, R.D. Tolêdo Filho, H. Savastano Junior, "An investigation of bamboo shear test methods and the influence of heat on bamboo shear strength." *Construction and Building Materials*, vol. 399, p.132586, 2023.

[11] S.M. Dewi, A. Soehardjono, "The Strength of Axially Loaded Square Hollow-Section Column Made of Laminated Asian Bamboo (Dendrocalamus asper Becker)". *Research Journal of Applied Sciences, Engineering and Technology*, vol. 15(9), pp.337-343, 2018.

[12] W. Zhao, J. Zhou, Z. Long, Z., "Compression tests on square, thin-walled steel tube/bamboo-plywood composite hollow columns." *Science and Engineering of Composite Materials*, vol. 23(5), pp.511-522, 2016.

[13] C. Tan, H. Li, M. Ashraf, I. Corbi, O. Corbi, R. Lorenzo, "Evaluation of axial capacity of engineered bamboo columns." *Journal of Building Engineering*, vol. 34, p.102039, 2021.

[14] A.R. Rad, H. Burton, Y. Weinand, "Performance assessment of through-tenon timber joints under tension loads." *Construction and Building Materials*, 207, pp.706-721, 2019.

[15] S. Rapley, D.V. Bompa, S. Biswal, "Compression resistance of digitally fabricated hollow timber columns." *In Proceedings of IASS Annual Symposia*, 2023.

[16] C. Hong, H. Li, Z. Xiong, R. Lorenzo, I. Corbi, O. Corbi, D. Wei, C. Yuan, D. Yang, H. Zhang, "Review of connections for engineered bamboo structures." *Journal of Building Engineering*, vol. 30, p.101324, 2020.

[17] G.Y. Jeong, M.J. Park, J.S. Park, K.H. Hwang, "Predicting load-carrying capacity of dovetail connections using the stochastic finite element method." *Wood and Fiber Science*, pp.430-439, 2012.

[18] J. Jaaranen, G. Fink, "Experimental and numerical investigations of a timber-concrete dovetail splice joint." *Journal of Building Engineering*, vol. 43, p.103179, 2021.

[19] C. Robeller, Y. Weinand, "Fabrication-aware design of timber folded plate shells with double through tenon joints". *Robotic fabrication in architecture, art and design*, pp.166-177, 2016.

[20] J. Blaber, B. Adair, A. Antoniou, "Ncorr: open-source 2D digital image correlation Matlab software." *Experimental Mechanics*, vol. 55(6), pp.1105-1122, 2015.

[21] V. Nežerka, "Ncorr_post:DIC Post-Processing Tool", 2014. Available at: Ncorr_post: DIC post-processing tool (cvut.cz) (Accessed: 01/03/2024)